

AD-E430397

12  
new

LEVEL III

AD

ADA 083290

TECHNICAL REPORT ARBRL-TR-02217

NUMERICAL SIMULATION OF  
HYDRODYNAMIC RAM

Kent D. Kimsey

February 1980

DTIC  
ELECTE  
APR 22 1980  
S D  
E



US ARMY ARMAMENT RESEARCH AND DEVELOPMENT COMMAND  
BALLISTIC RESEARCH LABORATORY  
ABERDEEN PROVING GROUND, MARYLAND

Approved for public release; distribution unlimited.

DDC FILE COPY

80 4 7 175

Destroy this report when it is no longer needed.  
Do not return it to the originator.

Secondary distribution of this report by originating  
or sponsoring activity is prohibited.

Additional copies of this report may be obtained  
from the National Technical Information Service,  
U.S. Department of Commerce, Springfield, Virginia  
22151.

The findings in this report are not to be construed as  
an official Department of the Army position, unless  
so designated by other authorized documents.

*The use of trade names or manufacturers' names in this report  
does not constitute endorsement of any commercial product.*

UNCLASSIFIED

SECURITY CLASSIFICATION OF THIS PAGE (When Data Entered)

REPORT DOCUMENTATION PAGE		READ INSTRUCTIONS BEFORE COMPLETING FORM
1. REPORT NUMBER TECHNICAL REPORT ARBRL-TR-02217	2. GOVT ACCESSION NO. A083290	3. RECIPIENT'S CATALOG NUMBER
4. TITLE (and Subtitle) NUMERICAL SIMULATION OF HYDRODYNAMIC RAM	5. TYPE OF REPORT & PERIOD COVERED Final	
	6. PERFORMING ORG. REPORT NUMBER	
7. AUTHOR(s) Kent D. Kimsey	8. CONTRACT OR GRANT NUMBER(s)	
9. PERFORMING ORGANIZATION NAME AND ADDRESS US Army Ballistic Research Laboratory ATTN: DRDAR-BLT Aberdeen Proving Ground, MD 21005	10. PROGRAM ELEMENT, PROJECT, TASK AREA & WORK UNIT NUMBERS RDT&E 1L162618AH80	
11. CONTROLLING OFFICE NAME AND ADDRESS US Army Armament Research and Development Command US Army Ballistic Research Laboratory ATTN: DRDAR-BL Aberdeen Proving Ground, MD 21005	12. REPORT DATE FEBRUARY 1980	
	13. NUMBER OF PAGES 36	
14. MONITORING AGENCY NAME & ADDRESS (if different from Controlling Office)	15. SECURITY CLASS. (of this report) UNCLASSIFIED	
	15a. DECLASSIFICATION/DOWNGRADING SCHEDULE	
16. DISTRIBUTION STATEMENT (of this Report) Approved for public release; distribution unlimited.		
17. DISTRIBUTION STATEMENT (of the abstract entered in block 20, if different from Report)		
18. SUPPLEMENTARY NOTES		
19. KEY WORDS (Continue on reverse side if necessary and identify by block number) Hydrodynamic ram Kinetic energy penetrator Fuel cell simulator		
20. ABSTRACT (Continue on reverse side if necessary and identify by block number) The EPIC-2 code has been used for the simulation of a kinetic energy projectile, with an L/D (length to diameter) ratio of 3, impacting at normal obliquity a cylindrical fuel cell simulator. A discussion of the predicted hydrodynamic ram event is presented along with a comparison with experimental data.		

DTIC  
ELECTE  
S APR 22 1980 D

B

TABLE OF CONTENTS

	Page
LIST OF ILLUSTRATIONS . . . . .	5
I. INTRODUCTION . . . . .	7
II. NUMERICAL MODEL . . . . .	8
III. RESULTS AND CONCLUSIONS . . . . .	11
APPENDICES	
A. VELOCITY VECTOR MAPS . . . . .	19
B. COMPUTATIONAL GRID MAPS . . . . .	25
DISTRIBUTION LIST . . . . .	31

PRECEDING PAGE BLANK - NOT FILMED

ACCESSION for		
NTIS	Write Section	<input checked="" type="checkbox"/>
DDC	Buff Section	<input type="checkbox"/>
UNANNOUNCED		<input type="checkbox"/>
JUSTIFICATION		
BY		
DISTRIBUTION AVAILABILITY CODES		
Dist.	AVAIL	and / or SPECIAL
A		

LIST OF ILLUSTRATIONS

Figure	Page
1 $V_s - V_r$ curve for steel penetrator vs 2024-T3 aluminum . . . . .	9
2 Initial conditions of hydrodynamic ram simulation . . . . .	10
3 Pressure contour map, $t=10 \mu s$ . . . . .	12
4 Pressure contour map, $t=40 \mu s$ . . . . .	13
5 Pressure contour map, $t=100 \mu s$ . . . . .	14
6 Pressure contour map, $t=140 \mu s$ . . . . .	15
7 Pressure contour map, $t=180 \mu s$ . . . . .	16
A.1 Velocity vector map, $t=10 \mu s$ . . . . .	20
A.2 Velocity vector map, $t=40 \mu s$ . . . . .	21
A.3 Velocity vector map, $t=100 \mu s$ . . . . .	22
A.4 Velocity vector map, $t=140 \mu s$ . . . . .	23
A.5 Velocity vector map, $t=180 \mu s$ . . . . .	24
B.1 Computational grid map, $t=10 \mu s$ . . . . .	26
B.2 Computational grid map, $t=40 \mu s$ . . . . .	27
B.3 Computational grid map, $t=100 \mu s$ . . . . .	28
B.4 Computational grid map, $t=140 \mu s$ . . . . .	29
B.5 Computational grid map, $t=180 \mu s$ . . . . .	30

## I. INTRODUCTION

Hydrodynamic ram refers to the high pressures that are developed in a fluid when a fluid reservoir is penetrated by a K.E. (kinetic energy) projectile. Hydrodynamic ram in aircraft fuel cells can damage structural components or rupture tank walls which in turn can lead to fuel starvation, fire and explosion. Hydrodynamic ram is a paramount threat to today's combat aircraft.

The hydrodynamic ram event is generally considered to consist of a shock phase, a drag phase, a cavitation phase and an exit phase. The shock phase occurs during initial impact with the fluid at which time the projectile impulsively accelerates the fluid and generates an intense pressure field bounded by a hemispherical shock wave. This shock wave expands radially away from the impact point and may produce petaling of the entrance panel. As the projectile traverses the fluid it transfers a portion of its momentum to the fluid as it is decelerated due to viscous drag. If the projectile tumbles in the fluid, a significantly larger portion of the projectile's momentum will be transferred to the fluid. The radial velocities imparted to the fluid during the drag phase lead to the formation of a cavity behind the penetrator. This is often termed the cavitation phase. As the fluid seeks to regain its undisturbed condition, the cavity will oscillate. The time interval during which the exit panel of the fluid cell is perforated by the K.E. projectile is referred to as the exit phase. All of the above phases of hydrodynamic ram have been observed experimentally<sup>1-3</sup>. The collection of papers presented in Reference 4 provides a portrait of the state-of-the-art of analytical and empirical approaches to understanding the hydrodynamic ram phenomenon.

This report presents the results of a numerical simulation of a K.E. projectile with an L/D (length to diameter) ratio of 3 impacting at normal obliquity a cylindrical fuel cell simulator. Section II presents a description of the numerical model and Section III provides a discussion of the results and comparison with available experimental data.

---

<sup>1</sup>Ball, R. E., "Structural Response of Fluid-Containing-Tanks to Penetrating Projectiles (Hydraulic Ram) - A Comparison of Experimental and Analytical Results", Naval Postgraduate School, Monterey, California, NPS-57Bp78051, May 1976.

<sup>2</sup>Stepka, F.S. and Morse, C.R., "Preliminary Investigation of Catastrophic Fracture of Liquid-filled Tanks Impacted by High-Velocity Particles", NASA TN D1537, May 1963.

<sup>3</sup>Stepka, F.S., Morse, C.R., and Dengler, R.P., "Investigation of Characteristics of Pressure Waves Generated in Water Filled Tanks Impacted by High-Velocity Projectiles", NASA TN D1343, December 1965.

<sup>4</sup>Hydrodynamic Ram Seminar, University of Dayton, Dayton Ohio, May 1977, Technical Report AFFDL-TR-77-32.

## II. NUMERICAL MODEL

Dynamic analysis of a K.E. projectile penetrating a fluid-filled cylinder has been performed using the two-dimensional EPIC-2 code<sup>5</sup>. The hydrodynamic ram event simulated consists of an S7 steel penetrator with an L/D of 3 striking a cylindrical fuel cell simulator. The fuel cell walls are composed of 1.8mm of 2024-T3 Al with a tank depth of 15.24cm and an outside diameter of 50.8cm. The 50 gram, hemispherically capped projectile impacts the aluminum entrance panel with a striking velocity,  $V_s$ , of 914 m/s.

Initially the projectile was modeled as a deformable continuum. After perforating the entrance panel negligible deformation of the projectile could be detected. At later times, approximately 35  $\mu$ s, in the penetration process the projectile exhibited unrealistic distortions due to the finite elements adjacent to the penetrator "locking-up". This "locking-up" results from the artificially high hydrostatic pressure which is generated in elements that are severely distorted when the Mie-Gruneisen equation of state is used to predict hydrostatic pressures. This "locking-up" of water elements tends to transform the hemispherical cap into a conical cap at late times. Therefore, it was felt that a better numerical simulation would be obtained by modeling the penetrator as a nondeformable continuum.

The aluminum entrance panel offers negligible resistance to the steel penetrator which is modeled as a rigid body. The  $V_s$ - $V_r$  curve, which has been obtained using Lambert's equation<sup>6</sup>, shown in Figure 1 shows this to be an overmatch situation insofar as the fuel cell walls are concerned. Perforation of the entrance panel reduces the penetrator's velocity by less than one percent giving a residual velocity,  $V_r$ , of 909 m/s. In light of this "over-kill" condition a plug with a diameter slightly larger than one projectile diameter has been removed from the entrance panel, and the simulation has been initiated with the nose of the penetrator tangent to the fluid surface. The initial configuration of this hydrodynamic ram simulation is shown schematically in Figure 2.

EPIC-2 uses constant strain triangles to discretize a continuum and the hydrostatic pressure in a given element is computed using the Mie-Gruneisen equation of state. For this particular application of the EPIC-2 code the finite element model consists of 5424 elements and 2943 nodes. The fluid is simulated as water and sliding is permitted between the projectile and the water as well as between the water and the "wet" side of the entrance and exit panels.

<sup>5</sup>Johnson, G.R., "EPIC-2 A Computer Program For Elastic Plastic Impact Computations in 2 Dimensions Plus Spin", Honeywell Inc., Defense System Division, Contract Report ARBRL-CR-00373, June 1978. (AD #A058786)

<sup>6</sup>Lambert, J.P., "A Residual Velocity Predictive Model for Long Rod Penetrators, Ballistic Research Laboratory Report ARBRL-MR-02928, April 1978. (AD #B027660L)

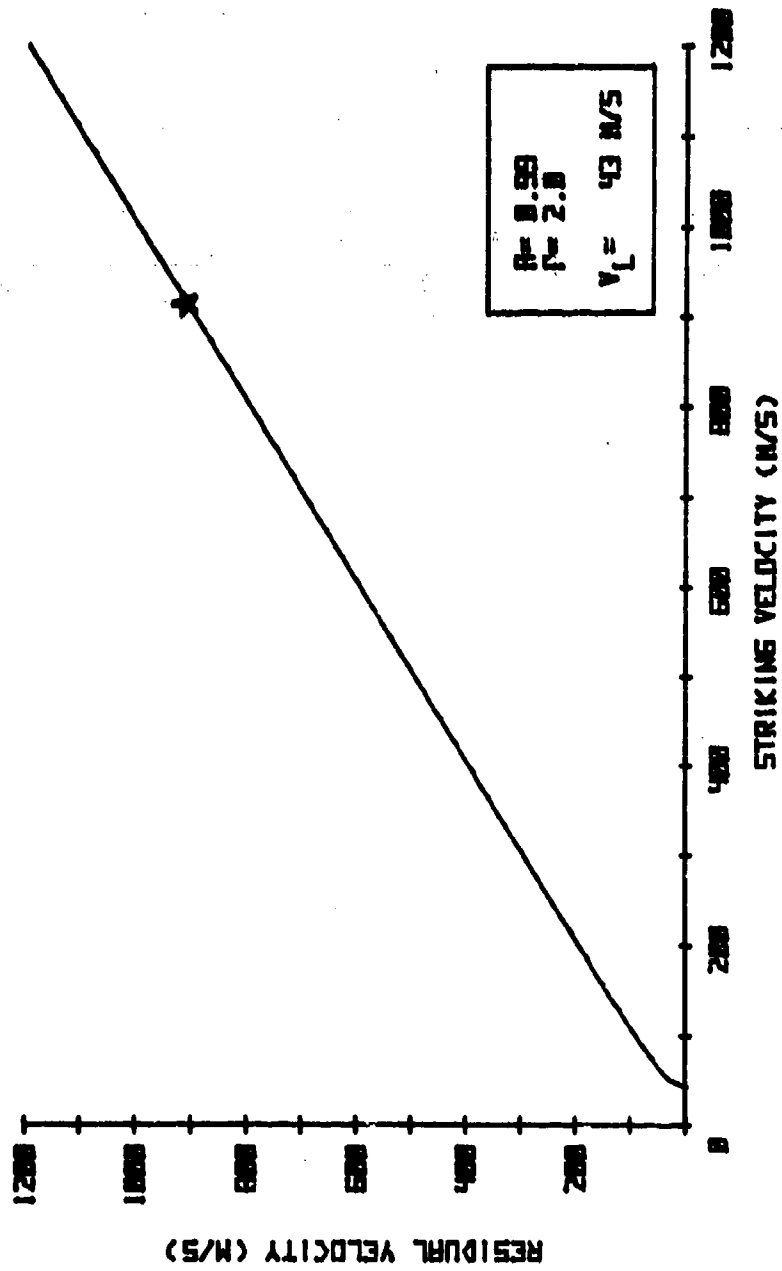
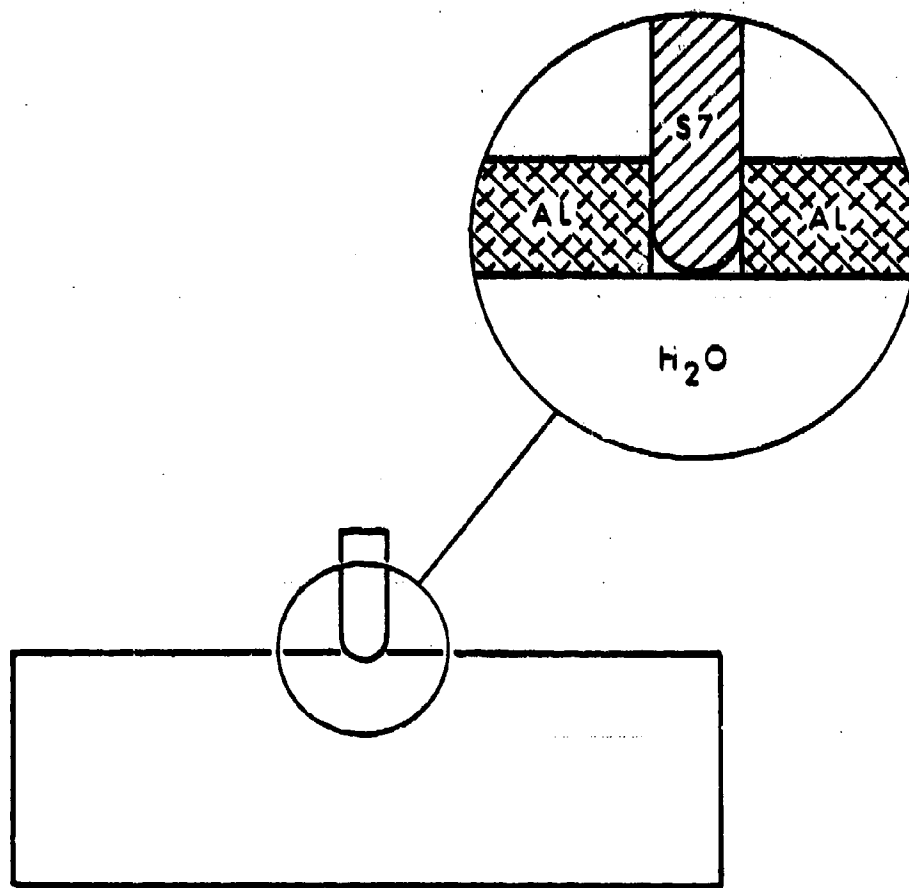


Figure 1.  $V_S$ - $V_T$  curve for steel penetrator vs 2024-T3 aluminum



PENETRATOR

S7 STEEL  
 L/D = 3  
 L = 4.26 cm  
 V<sub>0</sub> = 909 m/s  
 50 g

*NOT TO SCALE*

TANK

RIGHT CIRCULAR CYLINDER  
 O.D. = 50.8 cm  
 HEIGHT = 15.2 cm  
 WALLS - 2024-T3 AL  
 THICKNESS = 1.8 mm  
 FLUID - WATER

Figure 2. Initial conditions of hydrodynamic ram simulation

The sliding surface technique incorporated in the Lagrangian formulation of EPIC-2 evolves around the designation of master and slave nodes. The technique has the effect of assuming a frictionless surface. In the event a slave node penetrates a master surface element, during a given integration time increment, it is repositioned onto the master surface by conserving translational and rotational momenta and matching the slave node normal velocity with the normal velocity of the master surface at the location of the slave node<sup>5</sup>. For the hydrodynamic ram simulation the projectile has been designated the master surface and a column of water with a radius of 1.3 projectile radii running the entire tank depth, has been designated as slave nodes. Designation of the interior nodes of the water elements to be slave nodes permits the water elements to be completely failed (i.e. the element produces no stresses or pressures) upon exceeding an equivalent strain of 2.5, and permits the simulation of the eroding process or cavity formation of the hydrodynamic ram phenomenon.

### III. RESULTS AND CONCLUSIONS

All phases except the exit phase of the hydrodynamic ram event have been simulated with the EPIC-2 code. Figures 3 - 7 present a collage of pressure contour maps in the water. It should be noted that the analysis is an axisymmetric solution and the projectile is restrained from tumbling. Tumbling frequently occurs in experiments with small L/D ratios unless drag flares or other means of stabilization are provided.

The formation of a hemispherical shock wave is clearly delineated in Figure 3. This snap shot of the shock phase shows that slight petaling of the entrance panel has occurred as a result of the impulsive acceleration imparted to the entrance panel which has been observed in velocity vector maps, see Appendix A. The impulsive acceleration of the fluid during the shock phase generates peak pressures which are much higher (an order of magnitude) than those observed during the drag phase, see Figures 4 - 7. The duration of the pressure pulses generated during the drag phase is considerably longer than that observed during the shock phase.

The simulation has been terminated at 180  $\mu$ s at which time the exit panel has been sufficiently loaded to initiate bulging prior to perforation by the projectile. The entrance panel has been deflected considerably and an additional cavity between the entrance panel and the water has formed (Figure 7). The radial velocity imparted to the water (see velocity vector maps Appendix A) as the projectile penetrates the water leads to the formation of a cavity behind the projectile. The development of this cavity is portrayed in the computational grid maps in Appendix B. This cavity appears narrower than those which have been reported in the literature. However, quite frequently in experiments the projectile tumbles in the fluid thereby transferring more momentum to the fluid which generates a larger cavity than would be generated if the projectile did not tumble. Thus, for the axisymmetric solution presented here a narrow cavity prediction was anticipated.

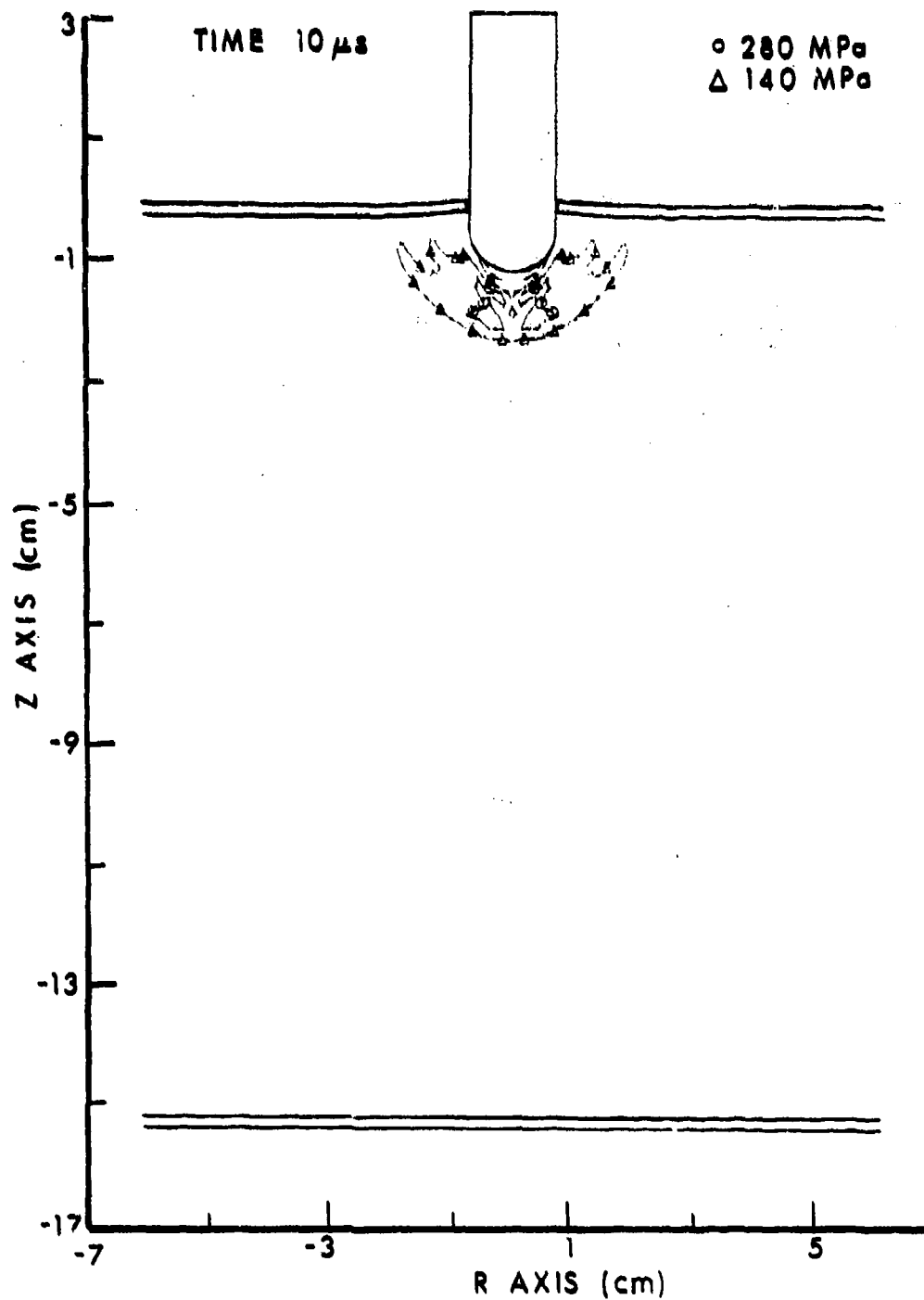


Figure 3. Pressure contour map,  $t=10 \mu$ s

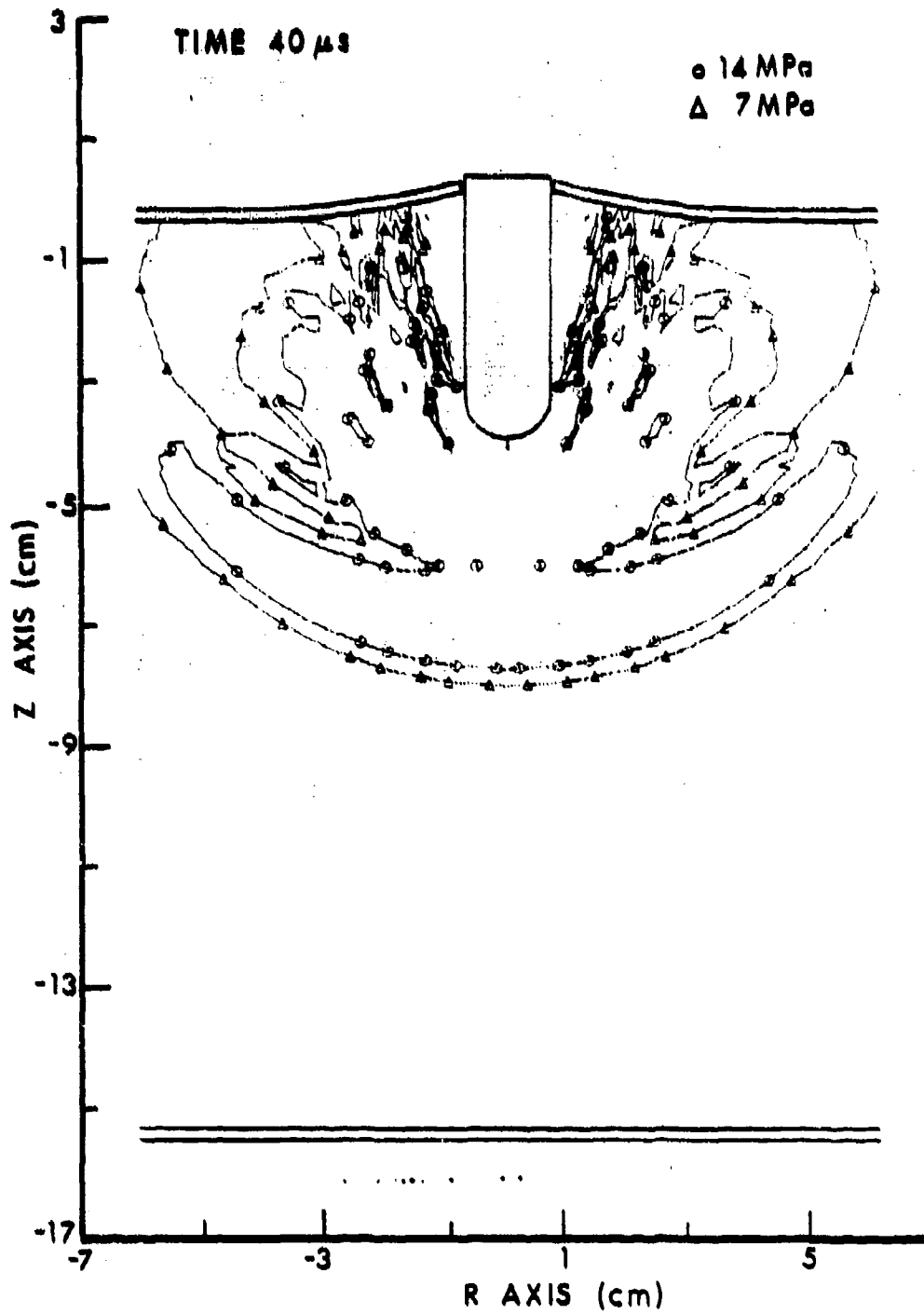


Figure 4. Pressure contour map,  $t=40 \mu$ s

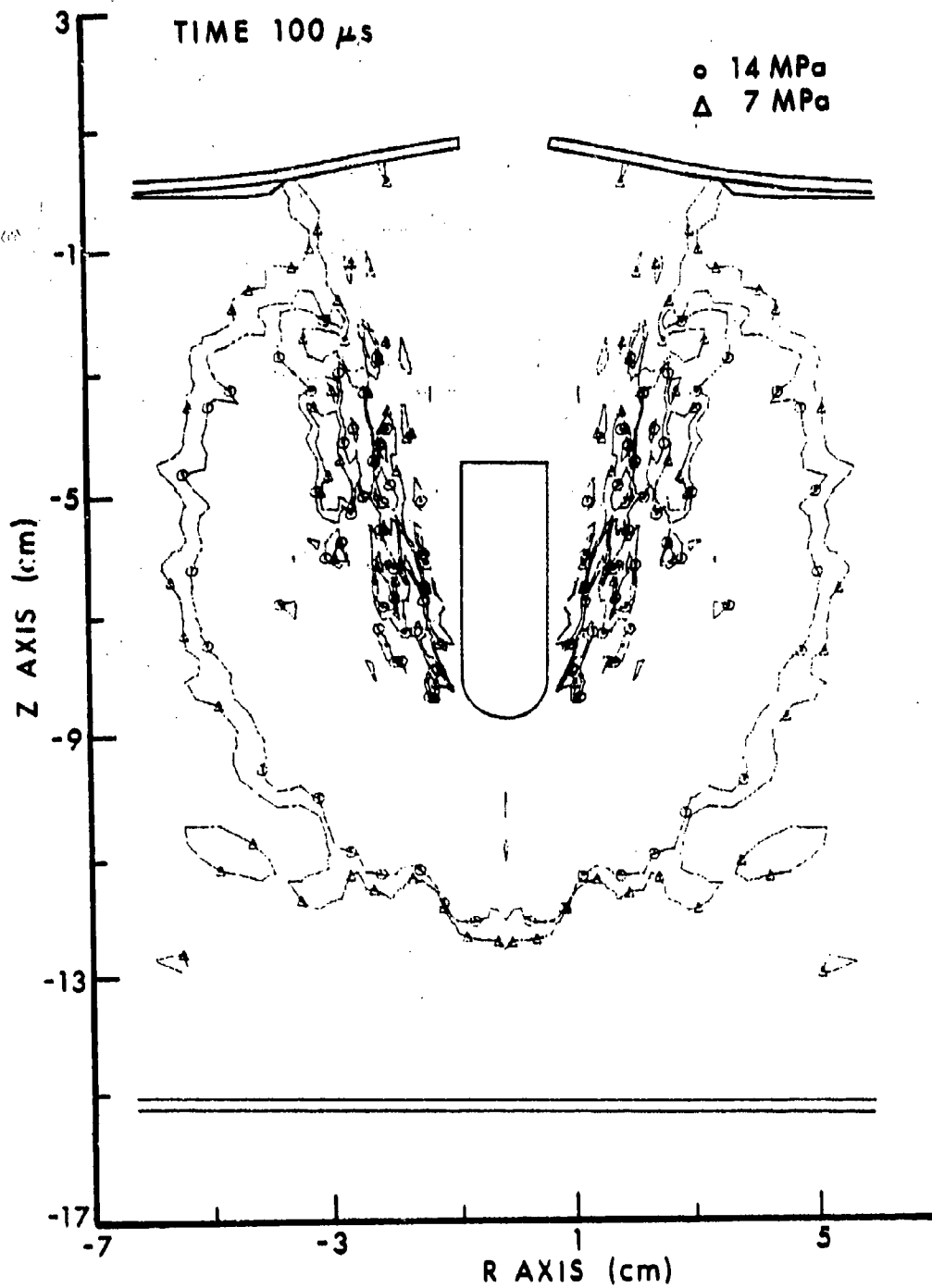


Figure 5. Pressure contour map,  $t=100 \mu$ s

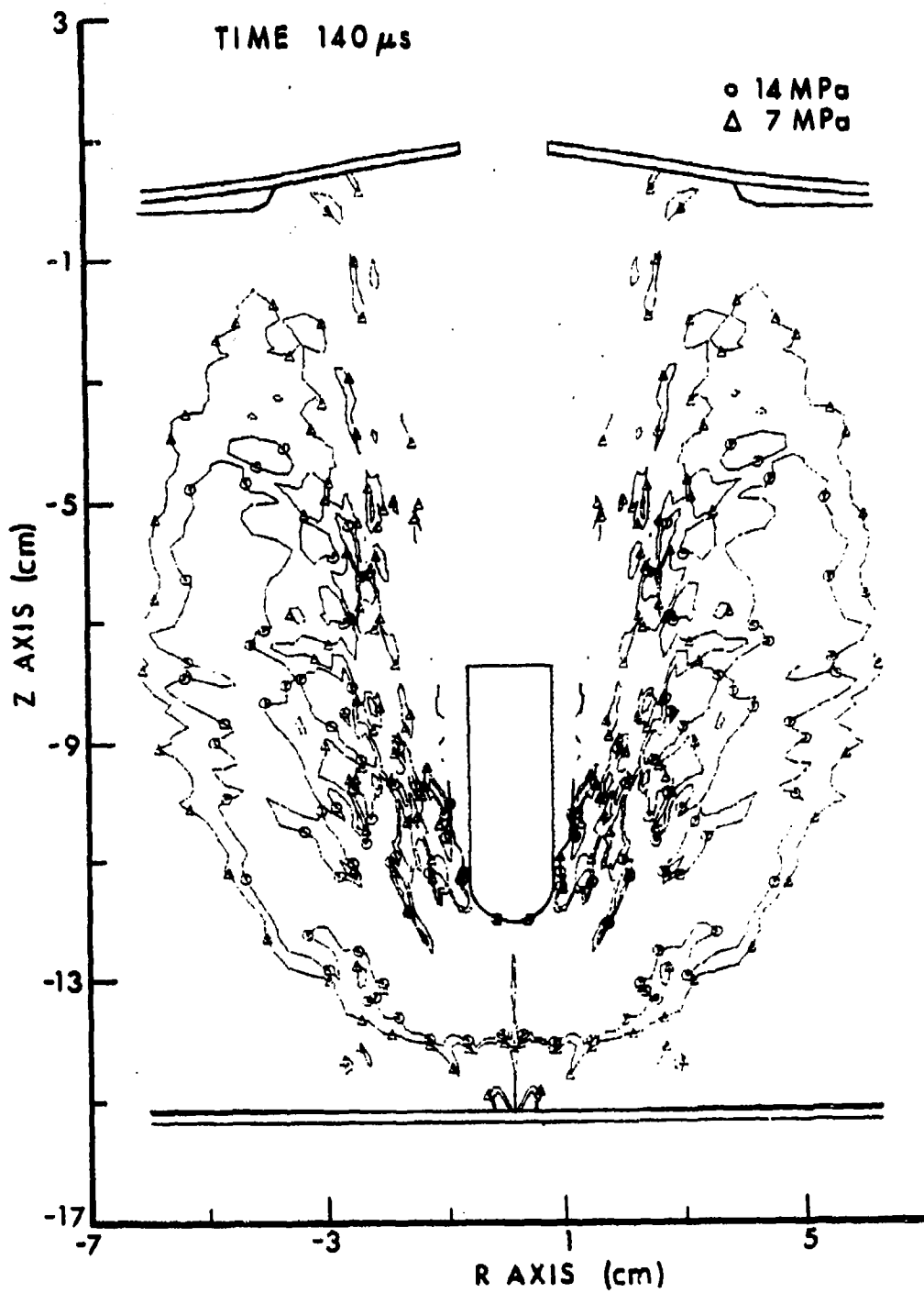


Figure 6. Pressure contour map,  $t=140 \mu$ s

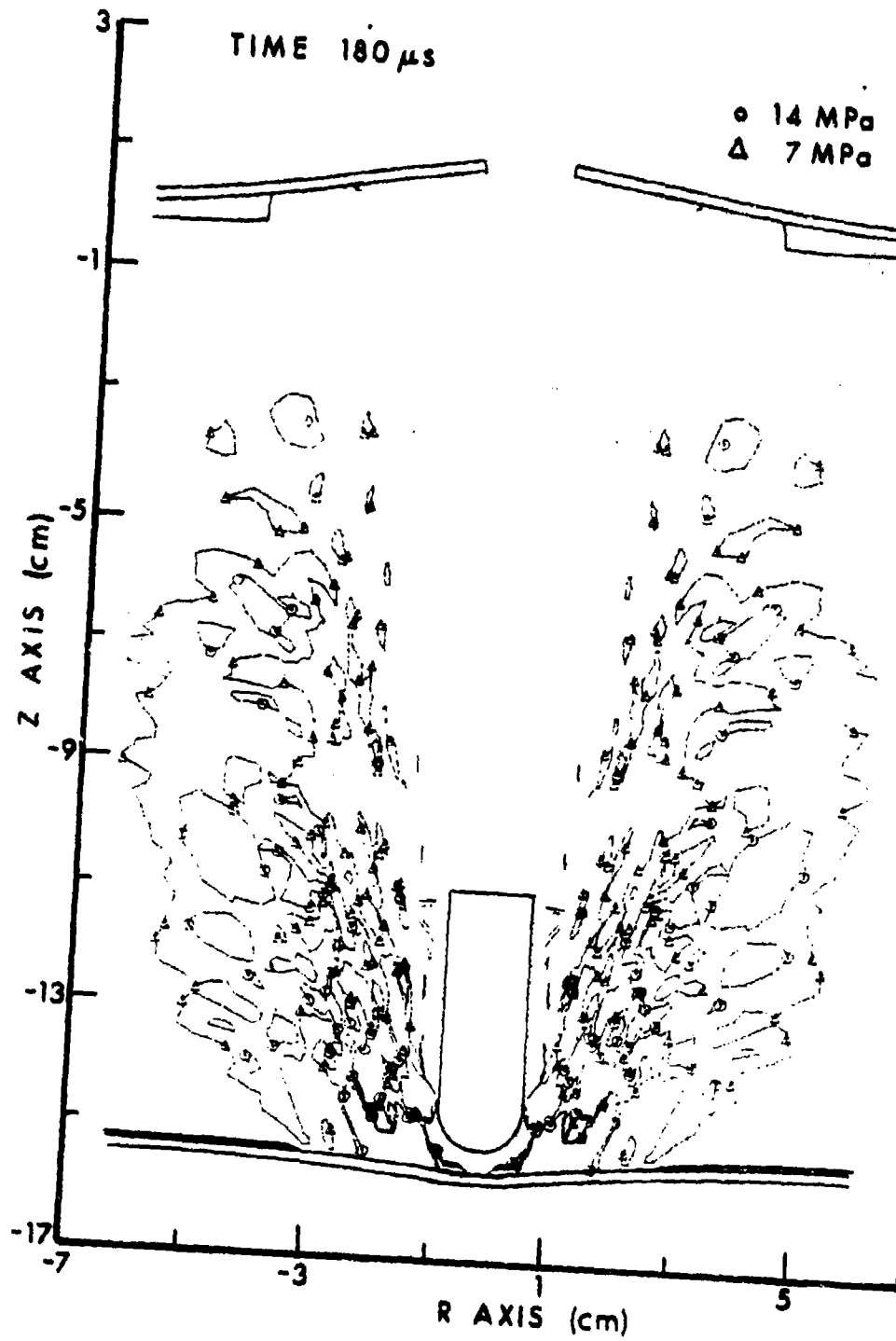


Figure 7. Pressure contour map,  $t=180 \mu$ s

The computational grid maps presented in Appendix B display those elements which have an equivalent strain less than 2.5. Elements which have undergone an equivalent strain greater than 2.5 are severely distorted and realistically would play no role in determining projectile response. These elements have therefore been eliminated or failed. Failure of an element implies that the element definition is destroyed, although the nodes and their associated mass and velocity are retained to conserve mass, energy, and momentum. Furthermore, those elements which have an "F" inside them identify those elements that have exceeded an equivalent strain of 0.02.

Reference 7 presents the following equation relating the striking and residual velocity of a projectile penetrating a water-filled container without tumbling:

$$\frac{V_R}{V_S} = e^{-\frac{C_D \rho_w t}{2 \rho_p L \cos \theta}} \quad (1)$$

where:

- $V_R$  - Residual velocity of the penetrator
- $V_S$  - Striking velocity of the penetrator
- $C_D$  - Drag coefficient of the penetrator
- $\rho_w$  - Density of the water
- $\rho_p$  - Density of the penetrator material
- $t$  - Effective separation distance of the entrance and exit panels of the tank
- $\theta$  - Obliquity angle
- $L$  - Penetrator length.

Equation (1) is used therein to compute residual velocities for a series of L/D of 5 projectiles penetrating 15.24cm of water. Striking velocities were reported to range from 0.9 km/s to 3 km/s and for tests at zero degrees obliquity, no appreciable change in angle of attack at the exit panel was observed. Generally, the calculated residual velocity was somewhat higher than the measured values, a discrepancy attributed to the projectile pitching slightly in the tank thereby increasing its drag coefficient.

---

<sup>7</sup>"Terminal Ballistics of Rod Penetrators," AVCO Systems Division, AVSD-0201-78-RR.

The drag coefficient for the L/D of 3, hemispherically capped projectile discussed in this report is estimated to be between 0.7 and 0.8<sup>8</sup>. These drag coefficients predict a 15% and a 17% reduction in projectile velocity respectively. At 180  $\mu$ s, see Figure 7, the projectile is near the exit panel and EPIC-2 predicts a 13.6% reduction in projectile velocity or a residual velocity of approximately 776 m/s. The projectile's velocity will be further reduced in penetrating the remaining fluid and the exit panel. The velocity decay predicted using EPIC-2 appears to be in line with that which has been measured in experiments with projectiles of similar design.

The use of EPIC-2 in understanding the hydrodynamic ram phenomenon looks promising. In this analysis EPIC-2 has confirmed that the entrance panel petaling results from the water impulsively accelerating the entrance panel, Figures 3 - 4. Furthermore, the hydrostatic pressures generated in the water initiate bulging of the exit panel prior to perforation by the projectile, Figure 7.

Additional damage can occur to the exit panel after it has been perforated by the projectile and a complete analysis of a hydrodynamic ram event should include the response of the exit panel until it reaches equilibrium. Perforation of the exit panel for the analysis presented here can be readily performed. Predicting the steady state response of the exit panel in this analysis would not be cost effective. The exit panel would reach a steady state condition in the millisecond regime while the integration time increment at 180  $\mu$ s is 72 nanoseconds. It is clear that it would take an unreasonable amount of computing time to predict the steady-state response of the exit panel. However, Reference 9 describes a time increment criterion based on the rate of deformation which would permit the total number of integration cycles to be dependent on the total amount of deformation and not the wave transit time across the minimum altitude of the most deformed element as is the case with the present explicit scheme in EPIC-2. Incorporation of such a strain rate dependent time increment criterion would make predicting the steady-state response of the exit panel feasible.

Numerical simulation to assess the influence of projectile yaw and tumbling on the hydrodynamic ram effect would have to be carried out with the three-dimensional version of the EPIC code<sup>10,11</sup>.

---

<sup>8</sup>Dr. P. Nietzel, private communication.

<sup>9</sup>Johnson, G. R., "Dynamic Analysis of Incompressible Viscous Fluids," *Journal of Applied Mechanics*, Vol 46, No 2, 1979.

<sup>10</sup>Johnson, G. R., "Further Development of the EPIC-3 Computer Program for Three-Dimensional Analysis of Intensive Impulsive Loading," AFATL-TR-78-81, July 1978.

<sup>11</sup>Johnson, G. R., "Further Development of EPIC-3 for Anisotropy, Sliding Surfaces Plotting and Materials Models," BRL Contractor Report to be published.

**APPENDIX A**  
**VELOCITY VECTOR MAPS**

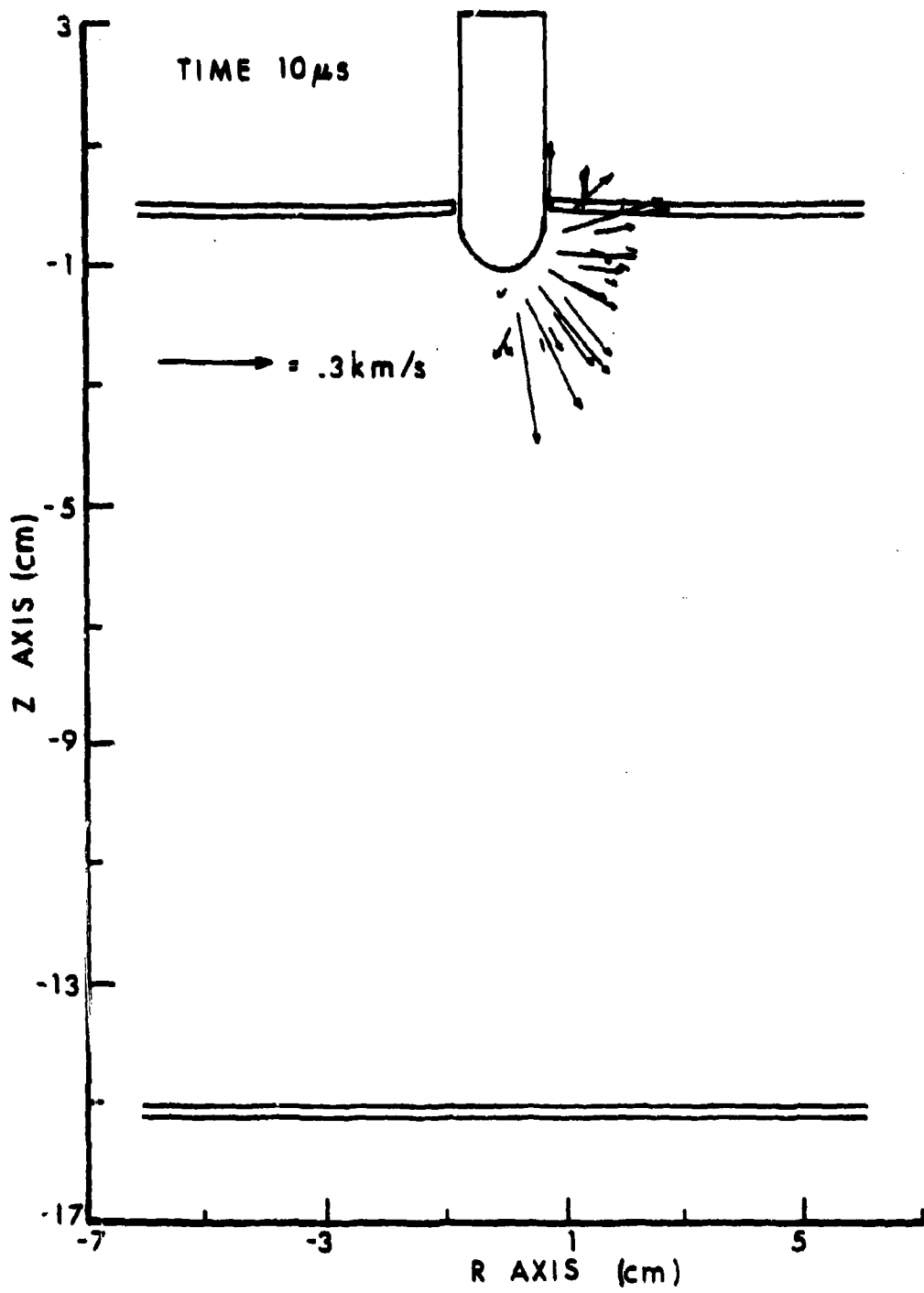


Figure A.1. Velocity vector map,  $t=10 \mu$ s

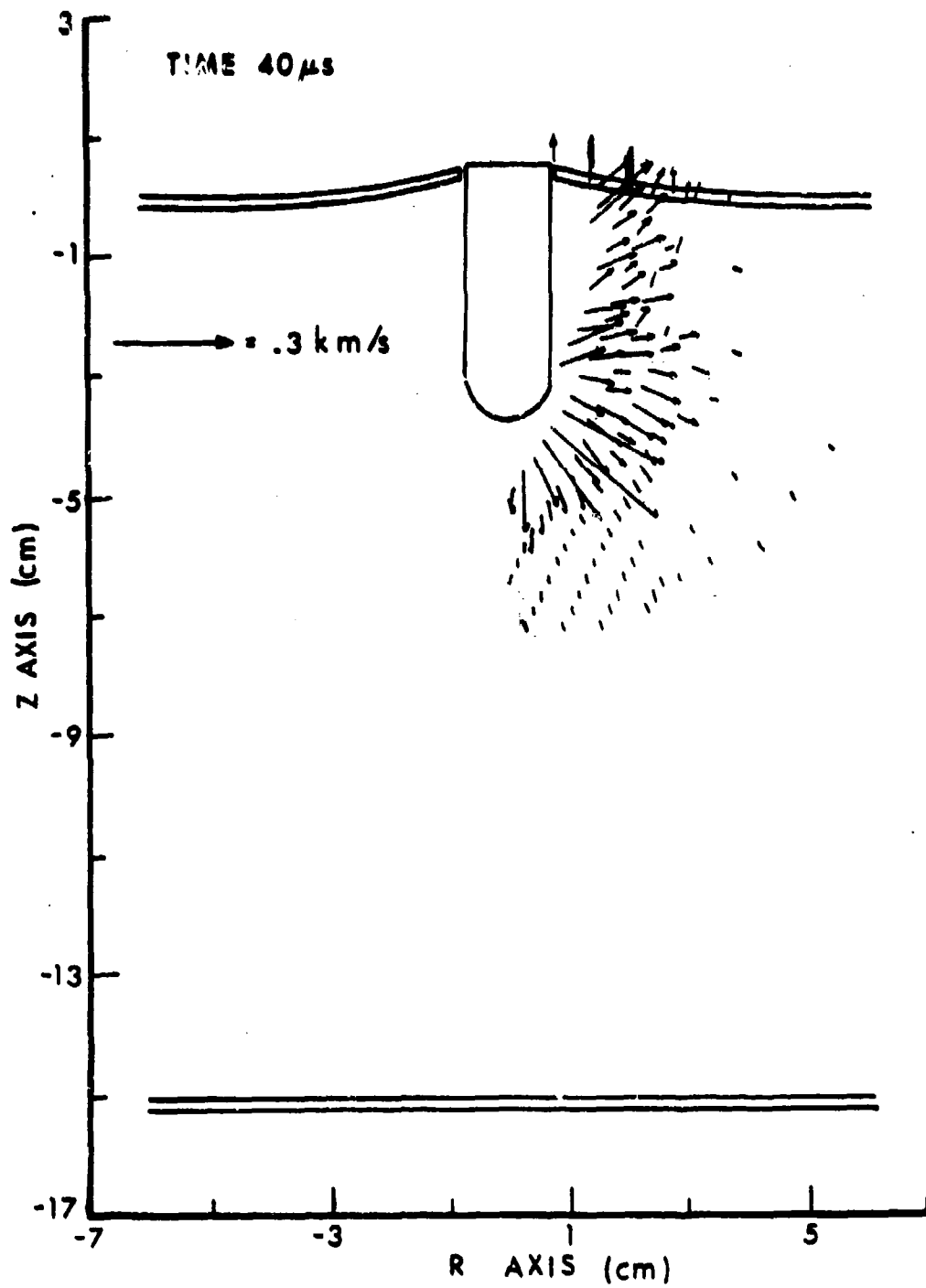


Figure A.2. Velocity vector map,  $t=40 \mu$ s

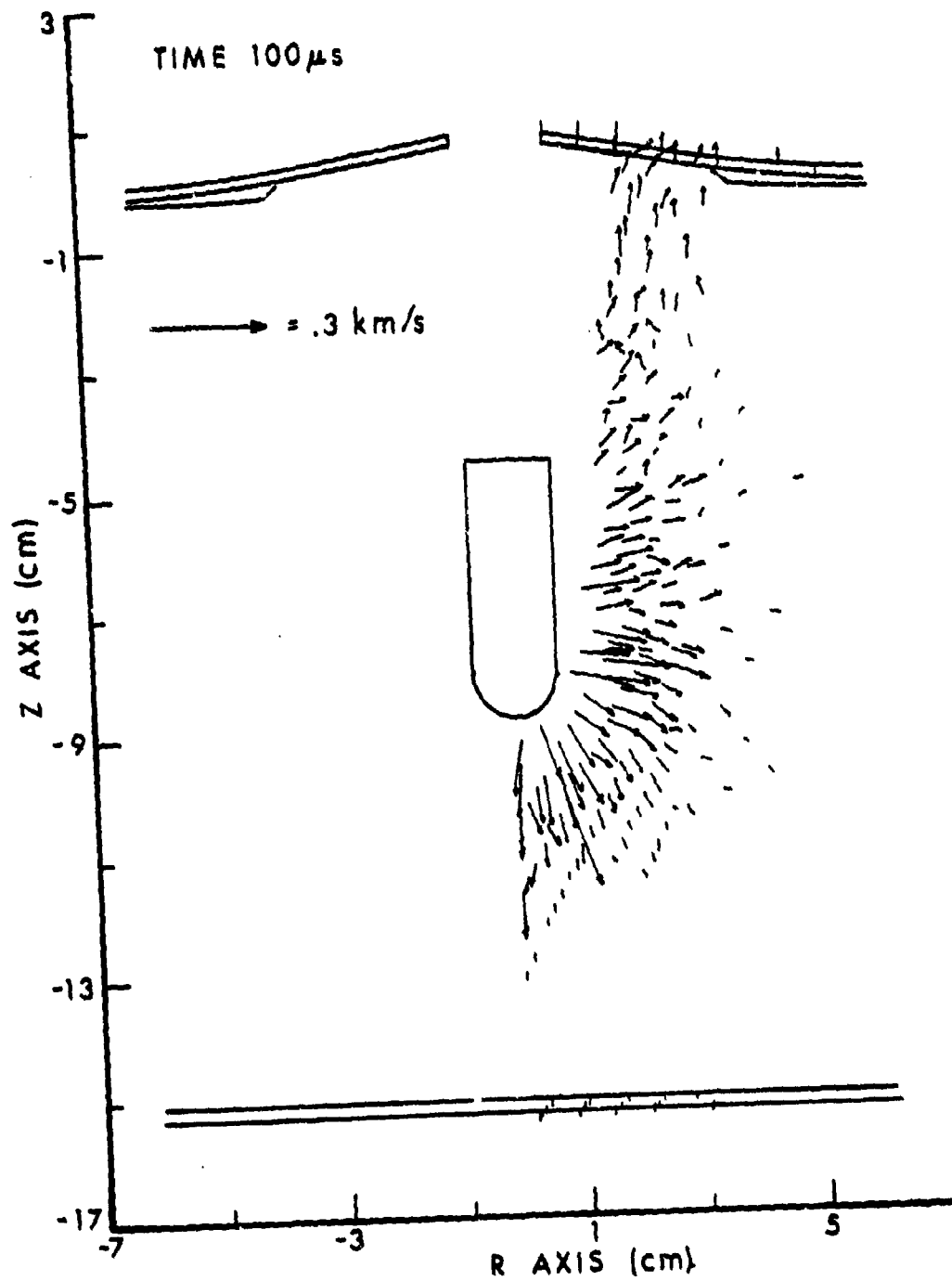


Figure A.3. Velocity vector map,  $t=100 \mu$ s

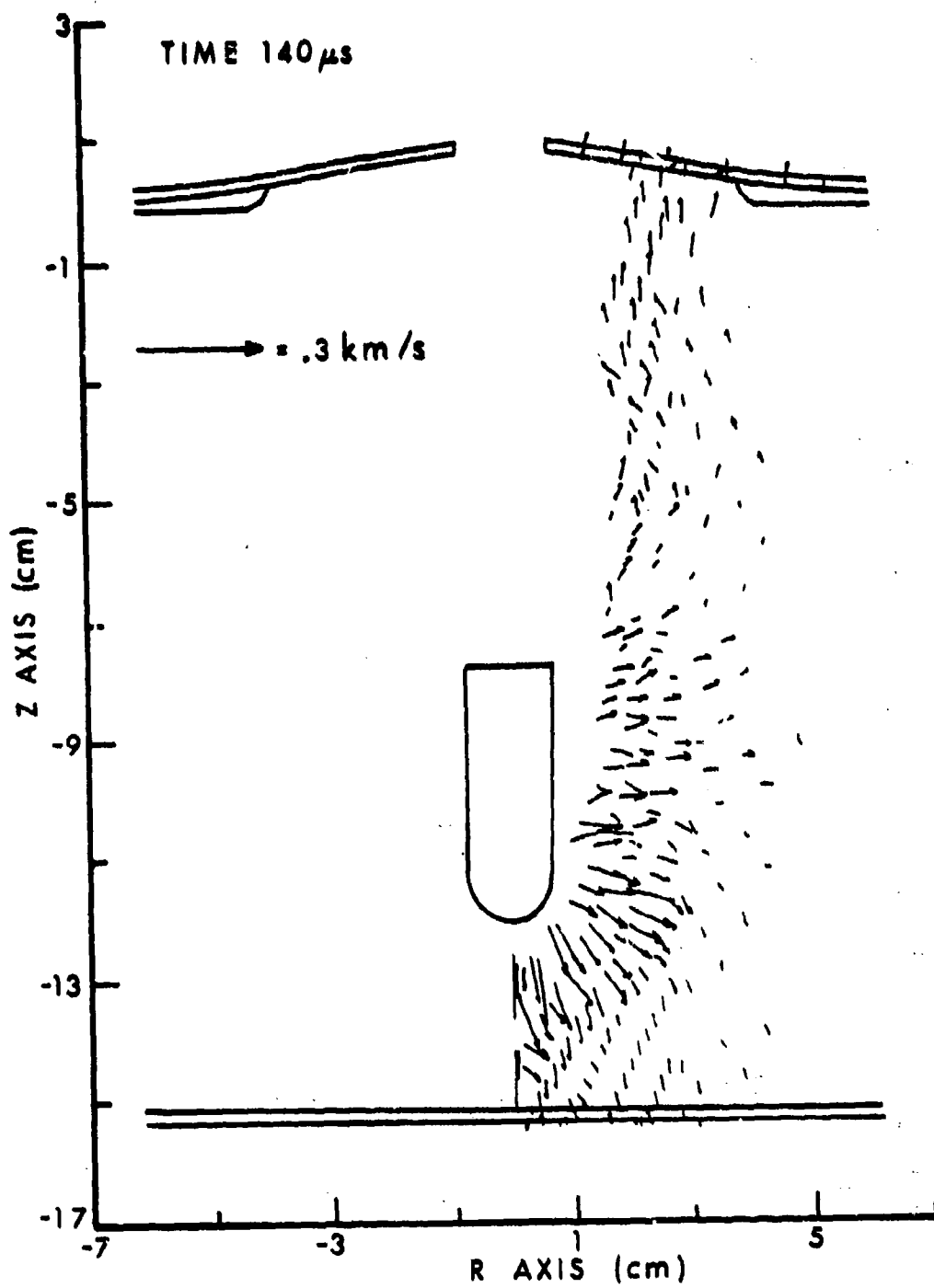


Figure A.4. Velocity vector map,  $t=140 \mu$ s

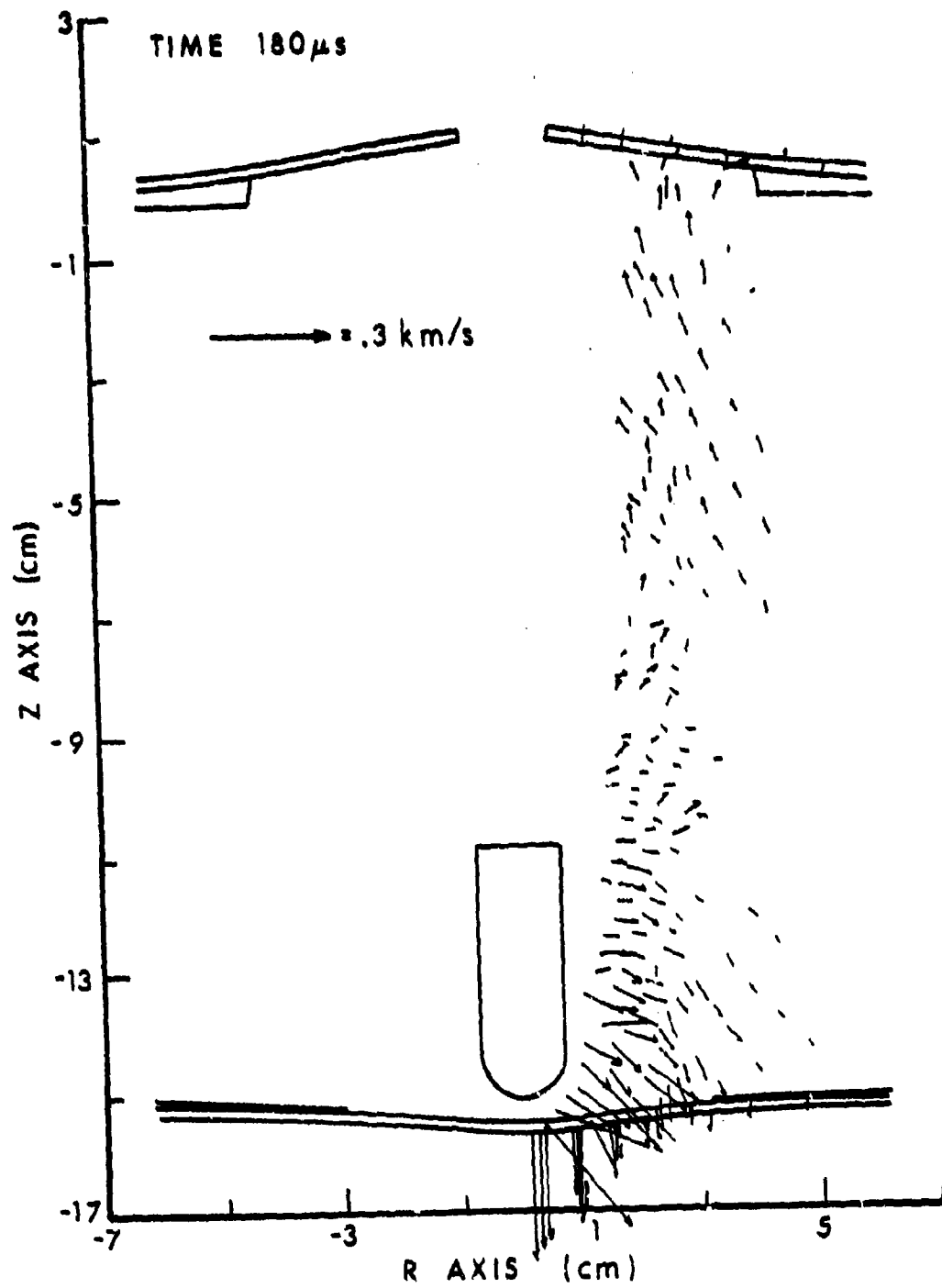


Figure A.5. Velocity vector map,  $t=180 \mu$ s

APPENDIX B  
COMPUTATIONAL GRID MAPS

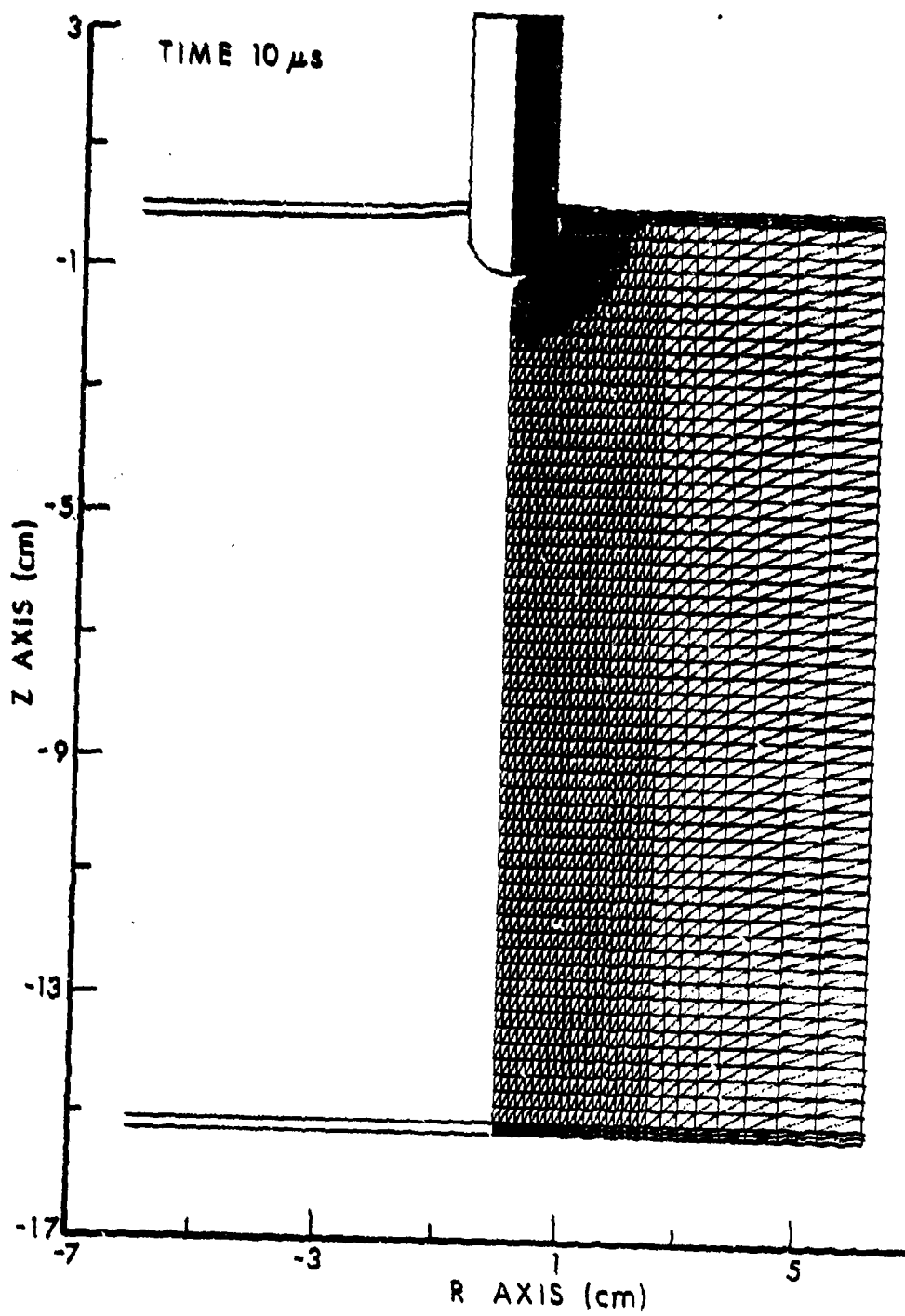


Figure B.1. Computational grid map,  $t=10 \mu s$

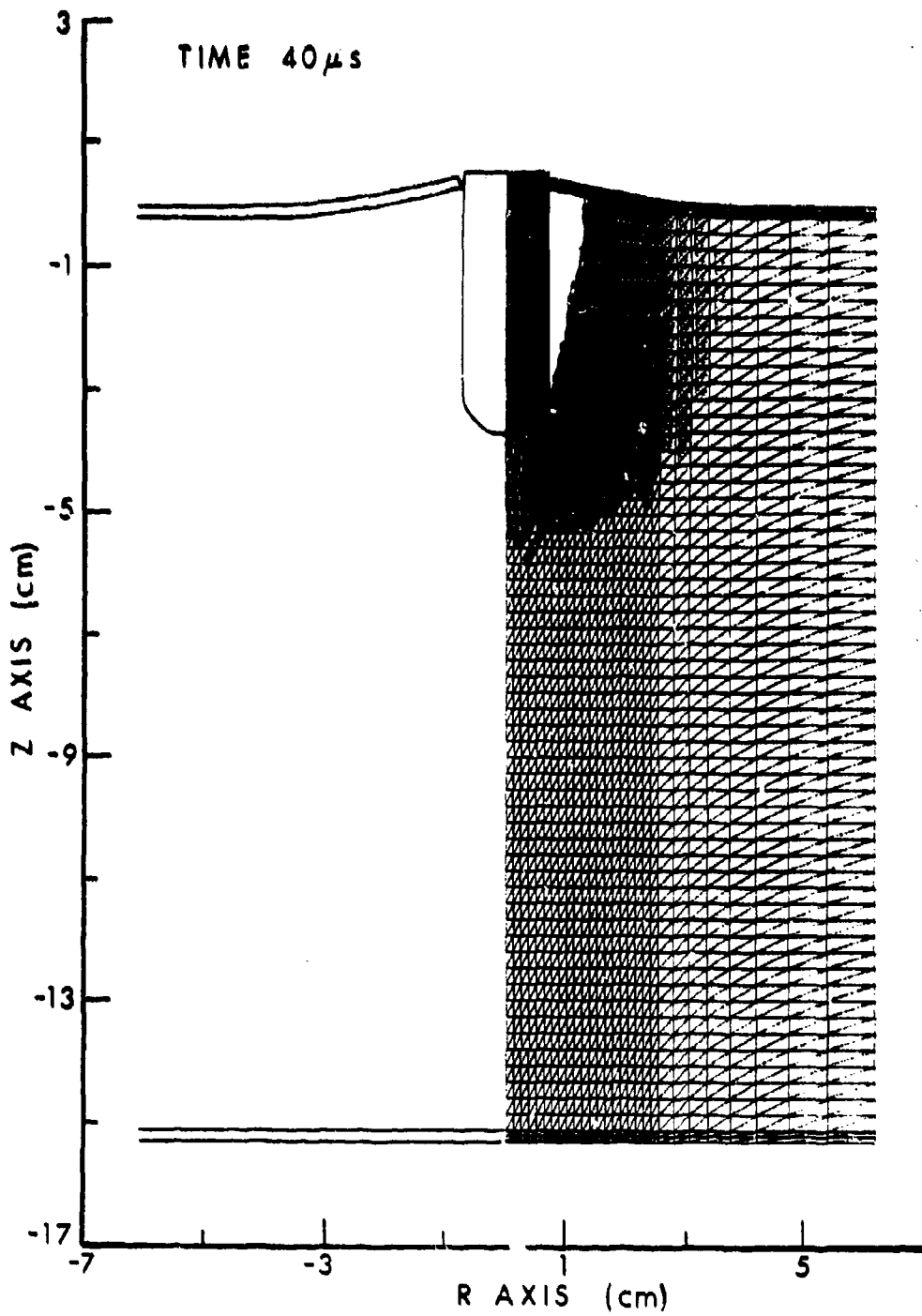


Figure B.2. Computational grid map,  $t=40 \mu$ s

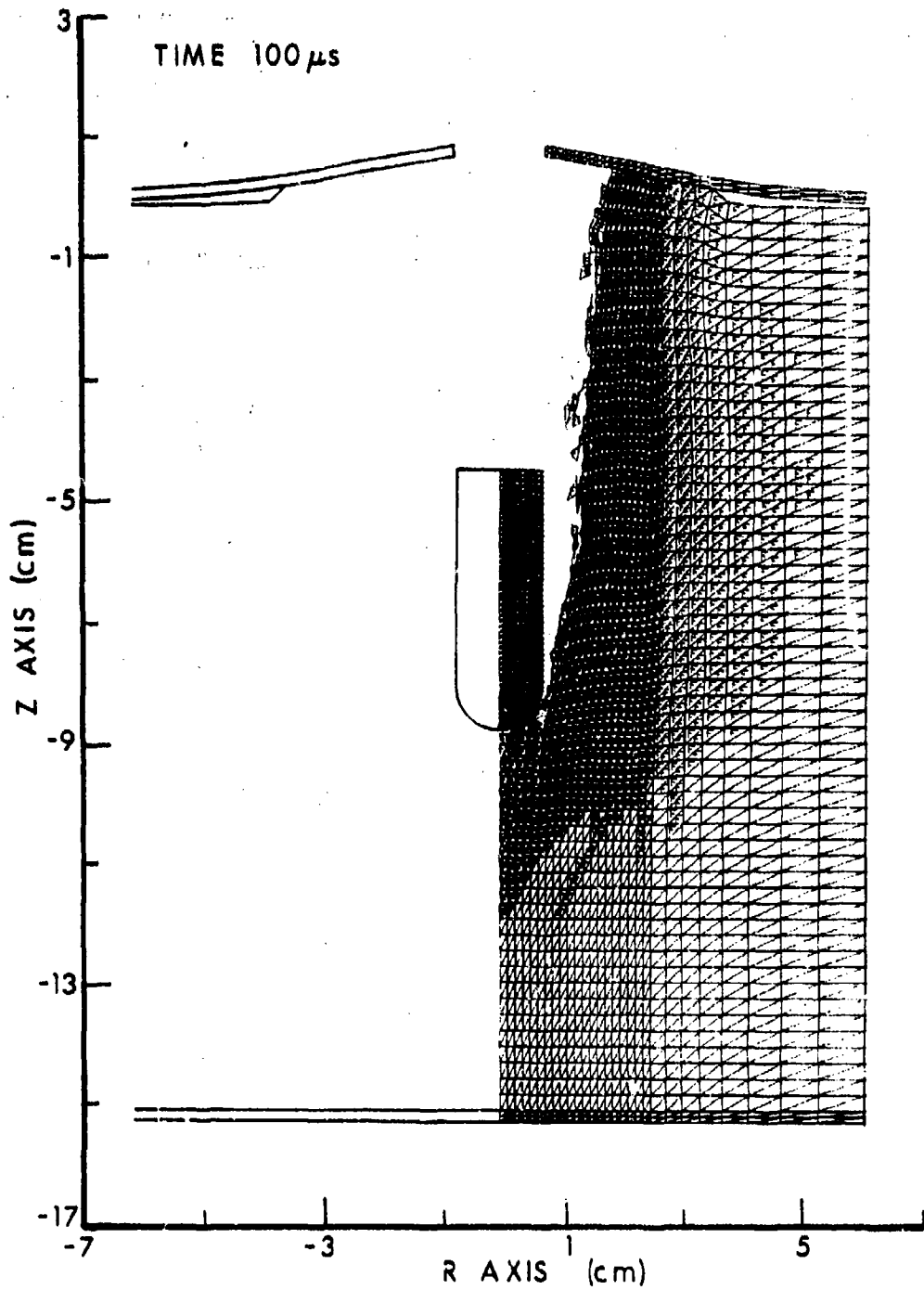


Figure B.3. Computational grid map,  $t=100 \mu$ s

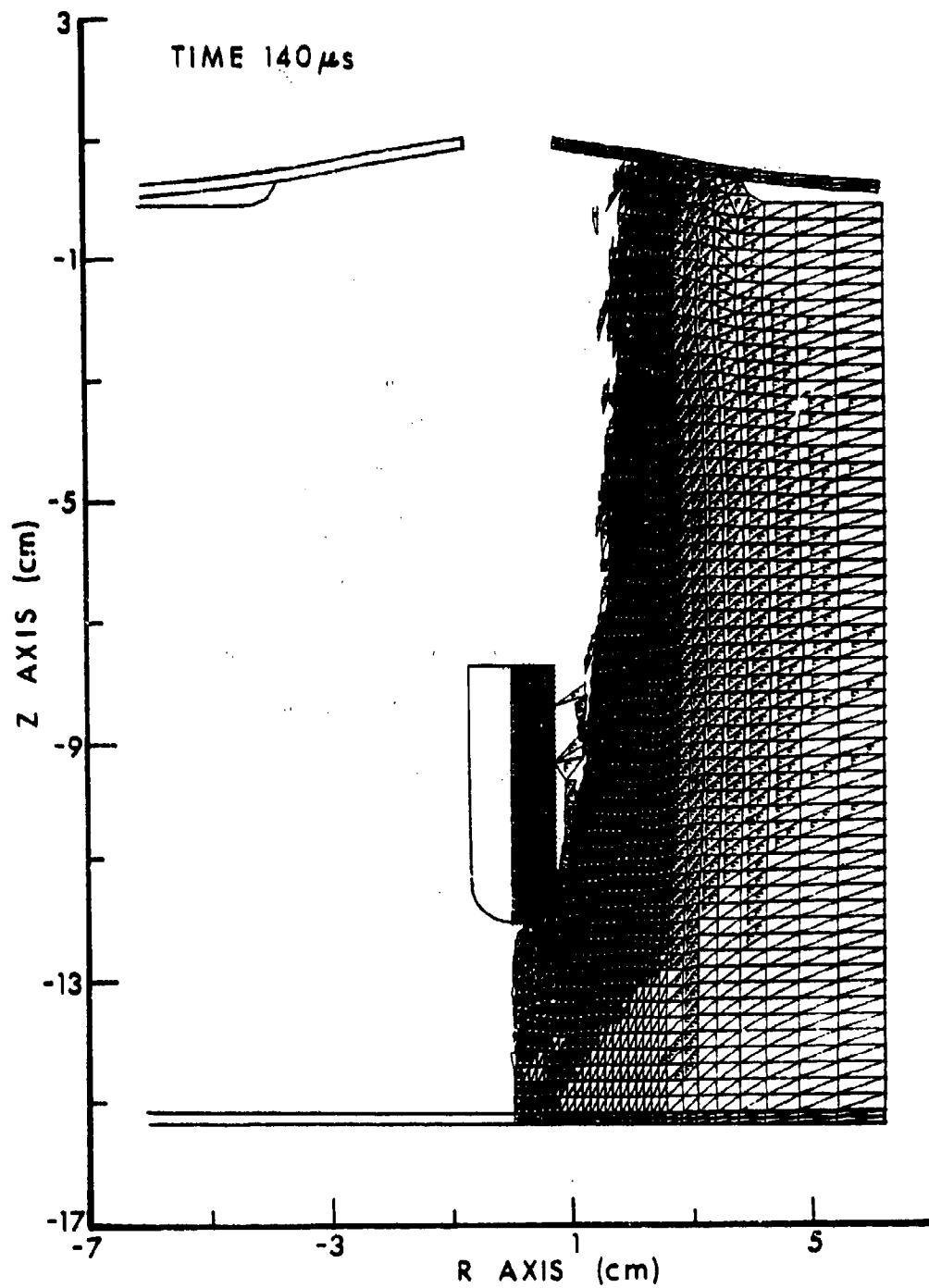


Figure B.4. Computational grid map,  $t=140 \mu$ s

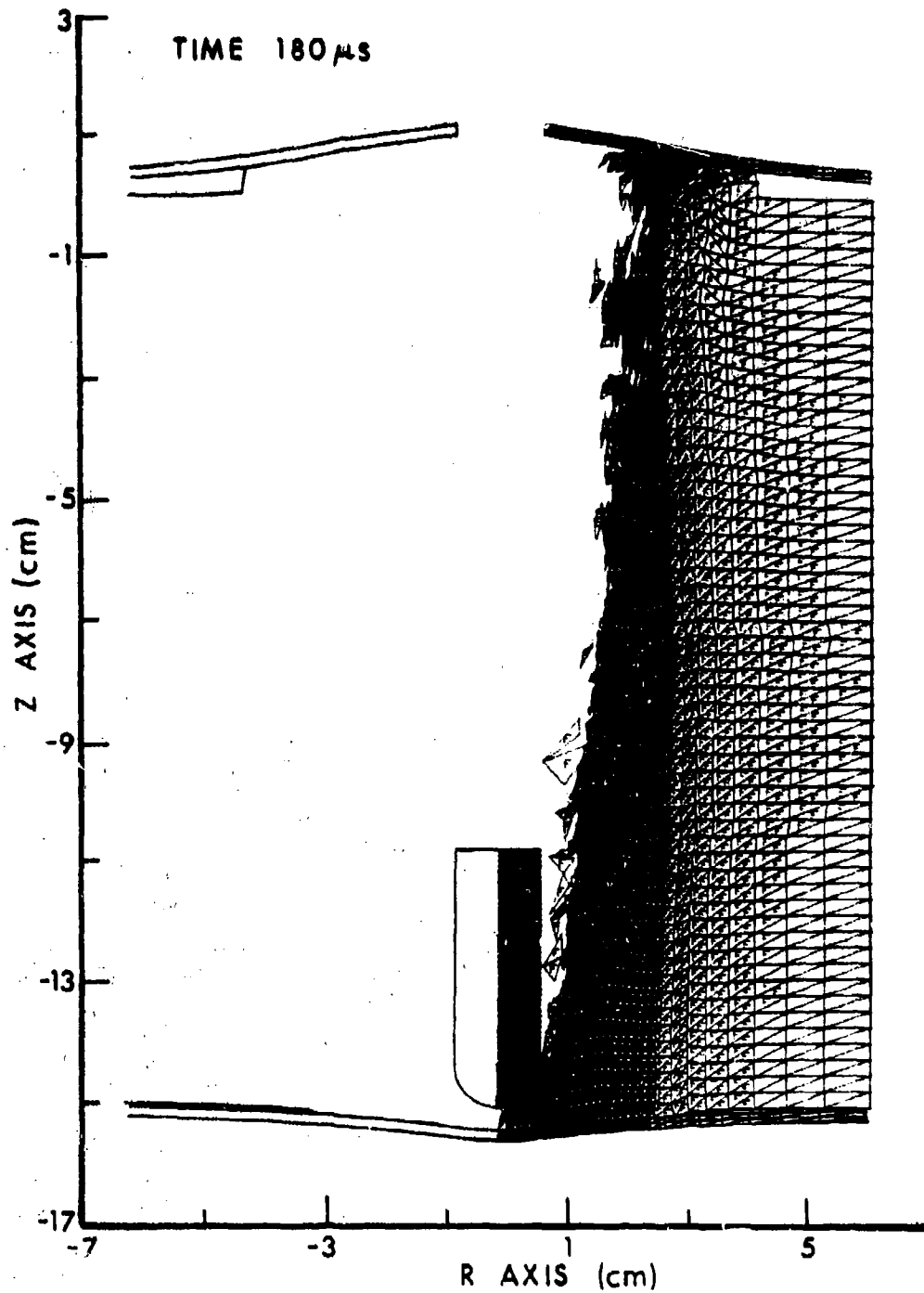


Figure B.5. Computational grid map,  $t=180 \mu$ s

DISTRIBUTION LIST

<u>No. of Copies</u>	<u>Organization</u>	<u>No. of Copies</u>	<u>Organization</u>
12	Commander Defense Technical Info Center ATTN: DDC-DDA Cameron Station Alexandria, VA 22314	1	Commander US Army Materiel Development and Readiness Command ATTN: DRCDMD-ST 5001 Eisenhower Avenue Alexandria, VA 22333
1	Director Defense Advanced Research Projects Agency ATTN: Tech Info 1400 Wilson Boulevard Arlington, VA 22209	5	Commander US Army Armament Research and Development Command ATTN: DRDAR-TD, Dr. R. Weigle DRDAR-LC, Dr. J. Frasier DRDAR-SC, Dr. D. Gyrog DRDAR-LCF, G. Demitrack DRDAR-LCA, G. Randers-Pehrson Dover, NJ 07801
1	Director Defense Nuclear Agency Arlington, VA 22209		
1	Deputy Assistant Secretary of the Army (R&D) Department of the Army Washington, DC 20310	6	Commander US Army Armament Research and Development Command ATTN: DRDAR-SCS-M, R. Kwatnoski DRDAR-SCA-T, H. Kahn P. Ehle DRDAR-LCU, E. Barrieres DRDAR-TSS (2 cys) Dover, NJ 07801
1	Commander US Army BMD Advanced Technology Center ATTN: BMDATC-M, Mr. P. Boyd PO Box 1500 Huntsville, AL 35807		
1	HQDA (DAMA-ARP) WASH DC 20310	1	Commander US Army Armament Materiel Readiness Command ATTN: DRSAR-LEP-L, Tech Lib Rock Island, IL 61299
1	HQDA (DAMA-MS) WASH DC 20310		
2	Commander US Army Engineer Waterways Experiment Station ATTN: Dr. P. Hadala Dr. B. Rohani PO Box 631 Vicksburg, MS 39180	1	Commander US Army Aviation Research and Development Command ATTN: DRSAV-E 12th and Spruce Streets St. Louis, MO 63166

**DISTRIBUTION LIST**

<u>No. of Copies</u>	<u>Organization</u>	<u>No. of Copies</u>	<u>Organization</u>
1	Director US Army Air Mobility Research and Development Laboratory Ames Research Center Moffett Field, CA 94035	1	Commander TARADCOM Tank-Automotive Systems Laboratory ATTN: T. Dean Warren, MI 48090
1	Commander US Army Communications Research and Development Command ATTN: DRDCO-PPA-SA Fort Monmouth, NJ 07703	7	Director US Army Materials and Mechanics Research Center ATTN: DRXMR-T, Mr. J. Bluhm Mr. J. Mescall Dr. M. Lencoe R. Shea CPT D. Riggs F. Quigley DRXMR-ATL Watertown, MA 02172
1	Commander US Army Electronics Research and Development Command Technical Support Activity ATTN: DELSD-L Fort Monmouth, NJ 07703		
2	Commander US Army Missile Research and Development Command ATTN: DRDMI-R DRDMI-RBL Redstone Arsenal, AL 35809	1	Commander US Army Research Office ATTN: Dr. E. Saibel Dr. G. Mayer PO Box 12211 Research Triangle Park NC 27709
1	Commander US Army Missile Research and Development Command ATTN: DRDMI-YDL Redstone Arsenal, AL 35809	1	Director US Army TRADOC Systems Analysis Activity ATTN: ATAA-SL (Tech Lib) White Sands Missile Range NM 88002
1	Commander US Army Tank-Automotive Re- search and Development Command ATTN: DRDTA-UL Warren, MI 48090	1	Office of Naval Research Department of the Navy ATTN: Code ONR 439, N. Perrone 800 North Quincy Street Arlington, VA 22217
1	Commander US Army Tank-Automotive Re- search and Development Command ATTN: V. H. Pagano Warren, MI 48090	3	Commander Naval Air Systems Command ATTN: AIR-604 Washington, DC 20360

DISTRIBUTION LIST

<u>No. of Copies</u>	<u>Organization</u>	<u>No. of Copies</u>	<u>Organization</u>
3	Commander Naval Ordnance Systems Command Washington, DC 20360	3	Commander Naval Research Laboratory ATTN: Dr. C. Sanday Dr. H. Pusey Dr. F. Rosenthal Washington, DC 20375
2	Commander Naval Air Development Center, Johnsville Warminster, PA 18974	2	Superintendent Naval Postgraduate School ATTN: Dir of Lib Dr. R. Ball Monterey, CA 93940
1	Commander Naval Missile Center Point Mugu, CA 93041	2	ADTC/DLJW (Mr. J. Collins/ Mr. W. Cook) Eglin AFB, FL 32542
2	Naval Ship Engineering Center ATTN: J. Schell Tech Lib Washington, DC 20362	1	AFATL/DLYV (W. S. Strickland) Eglin AFB, FL 32542
1	Commander & Director David W. Taylor Naval Ship Research & Development Center Bethesda, MD 20084	1	AFML/LLN (Dr. T. Nicholas) Wright-Patterson AFB, OH 45433
2	Commander Naval Surface Weapons Center ATTN: Dr. W. G. Soper Mr. N. Rupert Dahlgren, VA 22448	1	Lawrence Livermore Laboratory PO Box 808 ATTN: Ms. C. Westmoreland Livermore, CA 94550
2	Commander Naval Surface Weapons Center Silver Spring, MD 20910	1	Lawrence Livermore Laboratory PO Box 808 ATTN: Dr. M. L. Wilkins Livermore, CA 94550
7	Commander Naval Weapons Center ATTN: Code 31804, Mr. M. Keith Code 326, Mr. P. Cordle Code 3261, Mr. T. Zulkoski Code 3181, John Morrow Code 3261, Mr. C. Johnson Code 3171, Mr. B. Galloway Code 3831, Mr. M. Backman China Lake, CA 93555	1	Lawrence Livermore Laboratory PO Box 808 ATTN: Dr. R. Werne Livermore, CA 94550
		4	Los Alamos Scientific Laboratory PO Box 1663 ATTN: Dr. R. Karpp Dr. J. Dienes Dr. J. Taylor Dr. E. Fugelso Los Alamos, NM 87545

DISTRIBUTION LIST

<u>No. of Copies</u>	<u>Organization</u>	<u>No. of Copies</u>	<u>Organization</u>
3	Sandia Laboratories ATTN: Dr. W. Herrmann Dr. L. Bertholf Dr. A. Chabal Albuquerque, NM 87115	1	Computer Code Consultants 1680 Camino Redondo ATTN: Dr. Wally Johnson Los Alamos, NM 87544
1	Headquarters National Aeronautics and Space Administration Washington, DC 20546	1	Dupont Experimental Labs ATTN: Dr. Carl Zweben Wilmington, DE 19801
1	Director National Aeronautics and Space Administration Langley Research Center Langley Station Hampton, VA 23365	1	Effects Technology Inc 5383 Hollister Avenue PO Box 30400 Santa Barbara, CA 93105
1	Aeronautics Research Associates of Princeton, Inc 50 Washington Road Princeton, NJ 08540	2	Falcon R&D Thor Facility ATTN: Mr. D. Malick Mr. J. Wilson 696 Fairmount Avenue Baltimore, MD 21204
2	Aerospace Corporation 2350 E. El Segundo Blvd ATTN: Mr. L. Rubin Mr. L. G. King El Segundo, CA 90009	1	FMC Corporation Ordnance Engineering Div San Jose, CA 95114
2	Battelle Columbus Laboratories ATTN: Dr. M. F. Kanninen Dr. G. T. Hahn 505 King Avenue Columbus, OH 43201	1	General Electric Company Armament Systems Dept Burlington, VT 05401
1	Boeing Aerospace Company ATTN: Mr. R. G. Blaisdell (M.S. 40-25) Seattle, WA 98124	1	President General Research Corporation ATTN: Lib McLean, VA 22101
		1	Goodier Aerospace Corp 1210 Massillon Rd Akron, OH 44315
		1	H. P. White Laboratory 3114 Scarboro Road Street, MD 21154

### DISTRIBUTION LIST

<u>No. of Copies</u>	<u>Organization</u>	<u>No. of Copies</u>	<u>Organization</u>
3	Honeywell, Inc Government & Aerospace Products Division ATTN: Mr. J. Blackburn Dr. G. Johnson Mr. R. Simpson 600 Second Street, NE Hopkins, MN 55343	1	Science Applications Inc 101 Continental Blvd Suite 310 El Segundo, CA 90245
1	International Applied Physics, Inc 7546 McEwen Road ATTN: Mr. H. F. Swift Centerville, OH 45459	1	Ship Systems, Inc. 11750 Sorrento Valley Road ATTN: Dr. G. G. Erickson San Diego, CA 92121
1	Kaman Sciences Corp 1500 Garden of the Gods Road ATTN: Dr. P. Snow Colorado Springs, CO 80933	1	Systems, Science and Software, Inc PO Box 1620 ATTN: Dr. R. Sedgwick La Jolla, CA 92038
1	Lockheed Palo Alto Research Laboratory 3251 Hanover Street ATTN: Org. 5230, Bldg. 201 Mr. R. Roberson Palo Alto, CA 94394	1	US Steel Corp Research Center 125 Jamison Lane Monroeville, Pa 15146
1	Materials Research Laboratory Inc 1 Science Road Glenwood, IL 60427	1	Drexel University Department of Mechanical Engineering ATTN: Dr. P. C. Chou 32d and Chestnut Streets Philadelphia, PA 19104
2	McDonnell-Douglas Aeronautics Co 5301 Bolsa Avenue ATTN: Dr. L. B. Greszczuk Dr. J. Wall Huntington Beach, CA 92647	1	New Mexico Institute of Mining and Technology ATTN: TERA Group Socorro, NM 87801
1	Pacific Technical Corp 460 Ward Drive ATTN: Dr. F. K. Feldmann Santa Barbara, CA 93105	1	Forrestall Research Center Aeronautical Engineering Laboratory Princeton University ATTN: Dr. A. Eringen Princeton, NJ 08540

DISTRIBUTION LIST

<u>No. of Copies</u>	<u>Organization</u>	<u>No. of Copies</u>	<u>Organization</u>
3	Southwest Research Institute Department of Mechanical Sciences ATTN: Dr. U. Lindholm Dr. W. Baker Dr. R. White 8500 Culebra Road San Antonio, TX 78228	3	<u>Aberdeen Proving Ground</u>  Cdr, USATECOM ATTN: Mr. W. Pless Mr. S. Keithley DRSTE-TO-F  Dir, USAMSA ATTN: DRXSY-D DRXSY-MP, H. Cohen  Dir, Wpns Sys Concepts Team Bldg. E3516, EA ATTN: DRDAR-ACW
3	SRI International 333 Ravenswood Avenue ATTN: Dr. L. Seaman Dr. L. Curran Dr. D. Shockey Menlo Park, CA 94025		
2	University of Arizona Civil Engineering Department ATTN: Dr. D. A. DaDeppo Dr. R. Richard Tucson, AZ 86721		
1	University of California Department of Physics ATTN: Dr. Harold Lewis Santa Barbara, CA 93106		
2	University of Delaware Department of Mechanical Engineering ATTN: Prof. J. Vinson Dean I. Greenfield Newark, DE 19711		
1	University of Denver Denver Research Institute ATTN: Mr. R. F. Recht 2390 South University Boulevard Denver, CO 80210		

USER EVALUATION OF REPORT

Please take a few minutes to answer the questions below; tear out this sheet and return it to Director, US Army Ballistic Research Laboratory, ARRADCOM, ATTN: DRDAR-TSB, Aberdeen Proving Ground, Maryland 21005. Your comments will provide us with information for improving future reports.

1. BRL Report Number \_\_\_\_\_

2. Does this report satisfy a need? (Comment on purpose, related project, or other area of interest for which report will be used.)

\_\_\_\_\_  
\_\_\_\_\_  
\_\_\_\_\_

3. How, specifically, is the report being used? (Information source, design data or procedure, management procedure, source of ideas, etc.) \_\_\_\_\_

\_\_\_\_\_  
\_\_\_\_\_

4. Has the information in this report led to any quantitative savings as far as man-hours/contract dollars saved, operating costs avoided, efficiencies achieved, etc.? If so, please elaborate.

\_\_\_\_\_  
\_\_\_\_\_

5. General Comments (Indicate what you think should be changed to make this report and future reports of this type more responsive to your needs, more usable, improve readability, etc.) \_\_\_\_\_

\_\_\_\_\_  
\_\_\_\_\_

6. If you would like to be contacted by the personnel who prepared this report to raise specific questions or discuss the topic, please fill in the following information.

Name: \_\_\_\_\_

Telephone Number: \_\_\_\_\_

Organization Address: \_\_\_\_\_

\_\_\_\_\_  
\_\_\_\_\_